AC

KEK Preprint 94-25
May 1994
R

Implementation of the Doppler Broadening of a Compton-Scattered Photon into the EGS4 Code

Y. NAMITO, S. BAN and H. HIRAYAMA

Submitted to Nucl. Instrum. Meth.

National Laboratory for High Energy Physics, 1994

KEK Reports are available from:

Technical Information & Library
National Laboratory for High Energy Physics
1-1 Oho, Tsukuba-shi
Ibaraki-ken, 305
JAPAN

Phone: 0298-64-1171
Telex: 3652-534 (Domestic)
(0)3652-534 (International)
Fax: 0298-64-4604
Cable: KEK OHO
E-mail: LIBRARY@JPNKEKVX (Bitnet Address)
library@kekvax.kek.jp (Internet Address)

Implementation of the Doppler Broadening of a Compton-Scattered Photon into the EGS4 code

Y. NAMITO, S. BAN, H. HIRAYAMA

National Laboratory for High Energy Physics
Oho, Tsukuba-shi, Ibaraki-ken, 305, Japan

ABSTRACT

A modification to the general-purpose Monte Carlo electron-photon transport code EGS4[1] was made in order to include Doppler broadening of Compton-scattered photon energy due to electron pre-collision motion. The Compton- scattered photon energy is sampled from a cross-section formula based on the Compton profile, and the Compton scattering is sustained if the energy imparted to the electron is less than its binding energy. The electron binding effect modifies the scattered photon energy, angular distribution, and total cross section of the Compton scattering, and affects the photon mean free path used in the calculations. In the improved EGS4 code, all of these electron binding effects in Compton scattering are treated consistently. A simulation of 40 keV photon scattering by C and Cu samples was performed using the improved EGS4 code; the calculated scattered photon spectra agreed well with the measurements.

1. Introduction

The electron binding effect becomes apparent in Compton scattering when the photon energy is lower than a few hundred keV. It is necessary to take this binding effect into account when carrying out a precise simulation of low-energy photon transport, since the Compton scattering is one of the important phenomena in low-energy photon transport. The binding effect appears as a reduction in the total Compton-scattering cross section, and a modification of the angular distribution of the scattered photon: a reduction in the forward direction. The Compton-scattered photon energy is broadened by the pre-collision motion of the electron. Due to the electron binding effect, part of the broadened photon spectrum is suppressed. As is shown in the next section, modification of the angular distribution is obtained by integrating the broadened spectrum concerning the scattered photon energy; the reduced total Compton-scattering cross section is obtained by integrating the modified angular distribution of the Compton-scattered photon. Thus, the binding effects on the Compton-scattering total cross section, angular distribution, and scattered photon spectrum are different aspects of one phenomenum. Although including all of these three aspects consistently is the best way to treat the electron binding effect in Compton scattering, several authors treated it in a more simple way. One person studied the effect of the electron binding on the photon buildup factor by using the total Compton-scattering cross section of the bound electron.[2] Two authors[3] as well as Samili et al[4] implemented a modification of the angular distribution of the Compton-scattered photon into the EGS4 code using an incoherent scattering function. The same modification of the angular distribution of a Compton-scattered photon using an incoherent scattering function was implemented in SANDYL,[5] MCNP,[6] and ACCEPT[7] of the ITS series,[8] as well as several other Monte Carlo photon transport codes.[9,10] The authors' search of the literature revealed that two group of authors included the Doppler broadening of the Compton scattering into their Monte Carlo photon-transport code. Felsteiner and Pattison[11] included Doppler broadening in their Monte Carlo photon transport code in order to estimate a multiple-scattered photon in their Compton-profile measurement. In Felsteiner and Pattison's code, it is not clear whether the binding effects on the Compton-scattering total cross section, angular distribution, and scattered photon

spectrum were treated consistently or not, since no description was given regarding this point in ref. 11. The ACCEPT code mentioned above was also implemented the Doppler broadening of the Compton-scattered photon. In ACCEPT, the electron momentum distribution was expressed by a Gaussian function instead of a theoretically evaluated Compton profile, and the electron binding effect on the Doppler-broadened spectrum was included by uniformly reducing the spectrum instead of suppressing an energetically impossible part of the spectrum. While this approach was simple, agreement with the measurement shown in ref. 7 was not good.

In this study, the energy broadening of a Compton-scattered photon and suppression of the part of the broadened spectrum due to electron binding are implemented into the EGS4 code in order to precisely treat the Compton scattering by the bound electron. We adapted a method based on the Compton profile in order to treat the Doppler broadening. Regarding this point, our method is basically the same as that used in ref. 11. The electron binding effect modifies the scattered photon energy, angular distribution and total cross section of the Compton scattering, and affects photon mean free path used in the calculation. The advantage of this method is that all of these electron binding effects in Compton scattering are treated consistently. This consistency is important in some applications: for example, a low-energy photon buildup factor calculation. Another advantage of this method is it uses the general-purpose Monte Carlo code EGS4. The modification is immediately applicable for many applications: for example, a background spectrum estimation due to a scattered photon for X-ray apparatus, shielding, and a deep penetration calculation of a low-energy photon. The needs for a precise simulation of low-energy photon transport are increasing due to the recent increasing use of synchrotron radiation as well as the wide use of low-energy photon in medical applications.

2. Method of Calculation

The Compton-scattering computational routine of the EGS4 code was modified in order to consider the Doppler broadening of a scattered photon as well as the electron binding effect on it. Formulas related to the Compton scattering of a bound electron are briefly mentioned to show the relationship of the Doppler broadening, incoherent scattering function and total Compton cross section. A double-differential Compton-scattering cross section for a linearly polarized photon is prepared for this calculation by modifying the Ribberfors's formula in the relativistic impulse approximation:[12]

$$(\frac{d^2\sigma}{d\Omega dk})_{bC,i} = \frac{r_0^2}{4}(\frac{k_c k}{k_0^2})\frac{dp_z}{dk}(\frac{k_c}{k_0} + \frac{k_0}{k_c} - 2 + 4\cos^2\Theta)J_i(p_z), \tag{1}$$

where

$$p_z = -137\frac{k_0 - k - k_0 k(1-\cos\theta)/m_0c^2}{|\bar{k_0} - \bar{k}|}, \tag{2}$$

$$\frac{dp_z}{dk} = \frac{137k_0}{|\bar{k_0} - \bar{k}|k_c} - \frac{p_z(k - k_0\cos\theta)}{|\bar{k_0} - \bar{k}|^2}, \tag{3}$$

$$k_c = \frac{k_0}{1 + \frac{k_0}{m_0c^2}(1-\cos\theta)}, \tag{4}$$

$$|\bar{k_0} - \bar{k}| = \sqrt{k_0^2 + k^2 - 2k_0 k\cos\theta}. \tag{5}$$

Here , p_z is the projection of electron pre-collision momentum on the photon-scattering vector in atomic units, k_c is the Compton-scattered photon energy for an electron at rest, and θ is the scattering polar angle. The subscript "i" denotes the shell number, which corresponds to each (n,l,m)-th sub-shell. $J_i(p_z)$ is the Compton profile of the i-th shell,[13] r_o is the classical electron radius, and Θ is the angle between the incident polarization vector and the scattered polarization vector. Due to electron binding, the cross section given by eq.(1) is 0 when $k > k_0 - I_i$. Here, I_i is the binding energy of an electron in the i-th shell. Eq.(1) for two scattered

polarization vectors ($\bar{e_{\parallel}}$ and $\bar{e_{\perp}}$) is

$$
\begin{aligned}
(\frac{d^2\sigma}{d\Omega dk})_{bC,i,\parallel} &= \frac{r_0^2}{4}(\frac{k_c k}{k_0^2})\frac{dp_z}{dk}(\frac{k}{k_0}+\frac{k_0}{k}-2+4(1-\sin^2\theta\cos^2\phi))J_i(p_z), \\
(\frac{d^2\sigma}{d\Omega dk})_{bC,i,\perp} &= \frac{r_0^2}{4}(\frac{k_c k}{k_0^2})\frac{dp_z}{dk}(\frac{k}{k_0}+\frac{k_0}{k}-2)J_i(p_z).
\end{aligned}
\tag{6}
$$

Here, thinking of any unit vector in the plane normal to scattered propagation vector, that which maximizes the product with the incident polarization vector is $\bar{e_{\parallel}}$ and that which minimizes the product is $\bar{e_{\perp}}$. The equations used to calculate $\bar{e_{\parallel}}$ and $\bar{e_{\perp}}$ were derived by Namito, Ban and Hirayama.[14] By adding eq.(6) for two scattered polarization vector directions and averaging over the scattering azimuth angle (ϕ), the double-differential Compton cross section of a bound electron for unpolarized photon is obtained as:

$$
(\frac{d^2\sigma}{d\Omega dk})_{bC,i} = \frac{r_0^2}{2}(\frac{k_c k}{k_0^2})\frac{dp_z}{dk}(\frac{k_c}{k_0}+\frac{k_0}{k_c}-\sin^2\theta)J_i(p_z). \tag{7}
$$

By substituting eq.(3) into eq.(7) after eliminating the second term on the right-hand side of eq.(3), one obtains an equivalent formula to eq.(3) of ref. 12. The differential Compton cross section of a bound electron is obtained by integrating eq.(7) concerning k based on the assumption that $k = k_c$ in the second term on the right-hand side:

$$
(\frac{d\sigma}{d\Omega})_{bC,i} = \frac{r_o^2}{2}(\frac{k_c}{k_0})^2(\frac{k_c}{k_0}+\frac{k_0}{k_c}-\sin^2\theta)S_i^I(k_0,\theta,Z), \tag{8}
$$

where

$$
S_i^I(k_0,\theta,Z) = \int_{-\infty}^{p_{i,max}} J_i(p_z)dp_z. \tag{9}
$$

Here, Z is the atomic number and $S_i^I(k_0,\theta,Z)$ is the incoherent scattering function of the $i-th$ shell electrons in the impulse approximation calculated by Ribberfors and Berggren.[15] $S_i^I(k_0,\theta,Z)$ converges to the number of electrons in each sub-shell

when $p_{i,max} \rightarrow \infty$. The differential Compton cross section of one whole atom is obtained by summing eq.(9) for all of the sub-shells:

$$(\frac{d\sigma}{d\Omega})^{I}_{bC} = \frac{r_o^2}{2}(\frac{k_c}{k_0})^2(\frac{k_c}{k_0} + \frac{k_0}{k_c} - \sin^2\theta)S^I(k_0, \theta, Z), \tag{10}$$

where

$$S^I(k_0, \theta, Z) = \sum_i S^I_i(k_0, \theta, Z). \tag{11}$$

Here, $S^I(x, Z)$ is the incoherent scattering function of an atom in the impulse approximation. Another incoherent scattering function ($S^W(x, Z)$), based on Waller-Hartree theory[16] was widely used to treat the electron binding effect on the angular distrbution of a Compton-scattered photon. Here, x is the momentum transfer,

$$x = \frac{k_0[keV]}{12.399}\sin(\frac{\theta}{2}). \tag{12}$$

Using $S^W(x, Z)$, the differential Compton scattering cross section is

$$(\frac{d\sigma}{d\Omega})^{W}_{bC} = \frac{r_o^2}{2}(\frac{k_c}{k_0})^2(\frac{k_c}{k_0} + \frac{k_0}{k_c} - \sin^2\theta)S^W(x, Z). \tag{13}$$

The close agreement of $S^I(k_0, \theta, Z)$ and $S^W(x, Z)$ for several atoms was shown in ref.15. By integrating eq.(13) concerning Ω, the total bound Compton-scattering cross section of an atom is obtained,

$$\sigma_{bC} = \int^{4\pi} (\frac{d\sigma}{d\Omega})^{W}_{bC} d\Omega. \tag{14}$$

The photon mean free path is calculated using σ_{bC} instead of σ_{fC}(total free Compton scattering cross section). The relation of the total bound Compton cross section, incoherent scattering function, and the cut off in the Doppler-broadened Compton-scattered photon spectrum was shown.

In the improved Compton-scattering routine in the EGS4 code, the distance to the next photon interaction point is sampled using the photon mean free path, evaluated by σ_{bC} taken from the DLC-99/HUGO;[17,18] the probability of Compton

scattering in that interaction is calculated using σ_{bC}. After θ is sampled according to eq.(13) using $S^W(x, Z)$ taken from ref.17, the electron sub-shell number is sampled using the number of electrons in each sub-shell. Eq.(10) is not used to sample θ, since the validity of $S^I(k_0, \theta, Z)$ has not yet been tested for many conditions. Then, $p_{i,max}$ is calculated by putting $k = k_0 - I_i$ in eq.(2) for sampled θ. The p_z is sampled in the interval $[0, 100]$ using a normalized cumulative density function(c.d.f.) of $J_i(x)$

$$\xi = \frac{\int_o^{p_z} J_i(x)dx}{\int_0^{100} J_i(x)dx}. \tag{15}$$

Here, ξ is a random number between $[0, 1]$. The computer program used to prepare material data for EGS4 called PEGS4 was modified so as to calculate the right-hand side value of eq.(15). The PEGS4 was also modified in order to prepare incoherent scattering functions $S^W(x, Z)$ and σ_{bC}, and to calculate the photon mean free path using σ_{bC}. The speed down of Compton scattering routine in the improved EGS4 is negligible since sampling of p_z is carried out quickly by the c.d.f. method. When $p_z > p_{i,max}$, it is rejected, and the shell number "i" and p_z are sampled again. This sampling is continued until $p_z < p_{i,max}$ is satisfied. Then, another rejection by $\frac{k}{k_0}$, which corresponds to the second term on the right-hand side of eq.(7), is performed. Hereby the scattered photon energy (k) and polar angle (θ) were sampled according to eq.(7). When photon linear polarization is not considered, the scattering azimuth angle (ϕ) is sampled at random. When the photon linear polarization is considered, ϕ and the scattered polarization vector is calculated according to eq.(6). The details concerning the linearly polarized photon scattering in the EGS4 code is described in ref. 14. Accordingly, scattered-photon sampling following eq.(1) is performed. The Compton profile of a free atom is used. To treat a compound material, a mixture of free atoms is assumed and any molecular effect on the Compton profile is ignored. The Compton scattered electron energy is calculated using the energy conservation law and assuming that no energy absorption by atoms in the Compton scattering occurs.

3. Comparison with Measurements

A mono-energy photon-scattering experiment was performed at a BL-14C in a 2.5 GeV synchrotron light facility (KEK- PF) to measure the incoherent scattering function $S(x, Z)$.[19] Two measurements in this experiment were simulated using the improved EGS4 code.

The experimental arrangement is shown in Fig.1. Photons from a vertical wiggler were used after being monochronized by a Si(1,1,1) double crystal monochrometer. A linearly polarized 40keV mono-energy photon beam (degree of polarization, $P = 0.85$) was scattered by a sample located at point O with its normal vector $(-\frac{1}{2}, -\frac{1}{\sqrt{2}}, \frac{1}{2})$; the scattered photons were detected by two high-purity Ge detectors located at $\theta = 90°$. One Ge detector (Ge_2) was located in the plane of the incident polarization vector($\phi = 0°$), and the other (Ge_1) in the plane perpendicular to it ($\phi = 90°$). Samples were contained in a vacuum chamber, and vacuum pipes were placed between the vacuum chamber and the Ge detectors in order to reduce any scattering due to the air. Collimators of 5.01 mm aperture were placed in front of Ge detectors (C_1, C_2). The distance from the surface of the sample to the collimator was 434 mm. The opening angle of this collimator was 0.33° and the energy spread of a Compton-scattered photon due to this opening angle (without Doppler broadening) was negligibly small, 31eV in this measurement. The incident photon intensity was monitored in a free–air ionization chamber, which was calibrated using a calorimeter.[20] The C (t=0.589mm) and Cu (t=2mm) samples were chosen among various samples used, because the combination of a Doppler-broadened single Compton peak and a multiple-scattering component was obtained from the former sample and the electron binding effect appeared clearly in the spectrum from the later sample. The measured spectra are indicated by the closed circles in fig.2. The sharp peak at 40keV is due to Rayleigh scattering, and the broad peak at 37keV is due to Compton scattering. The average of measurements at $\phi = 90°$ and $\phi = 0°$ has been shown to clearly illustrate the effect of Doppler broadening. The flat part between 32 and 34 keV in fig.2(a) is the contribution due to multiple scattering. The binding effect of the K and L shell electrons of Cu appears as a drop near to 31 and 39keV, respectively in fig.2(b).

The calculation was carried out using the improved EGS4 code. The number

of cases followed in each calculation is 2×10^9 and the opening angle of 5° was used to score photons with sufficient statistics. The EGS4 calculation with all the modifications in this work (Doppler broadening, electron binding effect in Compton scattering, linearly polarized photon scattering) was carried out for C and Cu samples. The calculated photon spectra are smeared by a Gaussian function in order to account for the resolution of the Ge detectors. Both of measurement and calculation are absolute values *i.e.*, no normalization between the measurement and calculation was made. The results of the calculation are indicated by the solid histograms in figs.2(a) and (b). The agreement between the measurement and calculation is satisfying in both cases. A EGS4 calculation using all of the modifications described in this paper, except for Doppler broadening, was carried out in order to determine the effect of Doppler broadening. The result is shown by the dot-dash histogram in fig.2. The result of a calculation without considering Doppler broadening is apparently different from a measurement not only at the single Compton peak at 37keV, but also at multiple scattering components from 31 to 39 keV. In the result of a calculation without Doppler broadening for the C sample, two peaks exist at 31.8 and 38keV, which correspond to the energy loss of sequent 135° - 135° Compton scattering and 45° - 45° Compton scattering, respectively. In the result of the calculation without considering Doppler broadening for the Cu sample, the multiple-scattering component distributes mainly between 34.6 and 40keV, which correspond to the energy range of a single Compton scattering in any direction. Accordingly, this component is due to the contribution of photons which underwent single-Compton and single-Rayleigh scattering. This comparison clearly indicates the importance of the Doppler broadening in single and multiple Compton-scattering simulation. Due to the electron binding effect in Compton scattering, the 40keV photon mean free path in C and Cu are increased by 4.3 and 0.6%, respectively, and the 40keV photon total Compton-scattering cross section of C and Cu are decreased by 5.1 and 19%, respectively. In the comparison of Cu shown in fig.2(b), the K and L shell electron binding effect is well simulated. While the M and N shell electron binding is not apparent in the comparison, they should have some contribution to a lower energy calculation. Thus, all of the sub-shells were treated independently in this work.

4. Summary

The general-purpose Monte Carlo electron-photon transport code EGS4 was improved in order to treat the Doppler broadening of a Compton-scattered photon as well as the electron binding effect on it. Two mono energy photon-scattering measurements performed at KEK-PF were successfully simulated using the improved EGS4 calculations. Together with the Compton and Rayleigh scattering for a linearly polarized photon, a low-energy photon-transport simulation with a detailed scattering model using the EGS4 code becomes possible.

Acknowledgements: The authors express thanks to S. Tanaka, H. Nakashima, Y. Nakane, N. Sasamoto, Y. Sakamoto, and Y. Asano of the Japan Atomic Energy Research Institute (JAERI) and N. Nariyama of Ship Research Institute for their help in the experiment at KEK - PF. The author express thanks to J. B. Mann of Los Alamos National Laboratory who provide us with useful Compton profile data in microfilm form.

REFERENCES

1. W. R. Nelson, H. Hirayama, and D. W. O. Rogers, SLAC-265 (Stanford University, Stanford 1985).

2. H. Hirayama and D. K. Trubey, Nucl. Sci. Eng. 99 (1988) 145.

3. Y. Namito and H. Hirayama, "Improvement of low energy photon transport calculation by EGS4, Electron Bound Effect in Compton Scattering", Japan Atomic Energy Society, Osaka, March (1991).

4. A. Samili, C. Depeursinge, "Adaptation du code EGS: Implémentation de l'effet de liaison des électrons lors d'une diffusion Compton", Swiss Federal Institute of Technology, March (1991).

5. H. M. Colbert, "SANDYL A Computer Program for Calculating Combined Photon-Electron Transport in Complex Systems", SLL-74-0012,Sandia National Laboratory (1974).

6. "MCNP-A General purpose Monte Carlo Code for Neutron and Photon Transport", LA-739-M, (Rev.) Ver.2B, Los Alamos Monte Carlo Group, LANL(1981).

7. F. Cleri, Nucl. Instr. and Meth. A295 (1990) 231.

8. J. A. Halblcib and T. A. Mchorn, Nucl. Eng. 92 (1986) 338.

9. H. P. Chan and K. Doi, Phys. Med. Biol.28(1983)109.

10. J. F Williamson, F. C. Deibel and R. L. Morin, Phys. Med. Biol.29(1984)1063.

11. J. Felsteiner and P. Pattison, Phys. Rev. B 13 (1976) 2702.

12. R. Ribberfors, Phys. Rev. A 27 (1983) 3061.

13. F. Biggs, L. B. Mendelsohn and J. B. Mann, At. Data Nucl. Data Tables 16 (1975) 201.

14. Y. Namito, S. Ban and H. Hirayama Nucl. Instr. and Meth. A332 (1993) 277.

15. R. Ribberfors and K. F. Berggren, Phys. Rev. A 26 (1982) 3325.

16. I. Waller and D. R. Hartree, Proc. R. Soc. London, Ser. A 124 (1929) 124.

17. "DLC-99/HUGO, Package of Photon Interaction Data in ENDF/B-V Format", ORNL/ RSIC-46 (ENDF-335) Dec. (1983).

18. J. H. Hubbell et al, J. Phys. Chem. Ref. Data 4 (1975) 471.

19. Y. Namito et al, to be published.

20. H. Nakashima et al., Nucl. Instr. Meth. A310 (1991) 696.

FIGURE CAPTIONS

1) Experiment arrangement. A mono-energetic linearly polarized synchrotron radiation photon beam was scattered by a sample (S); the scattered photons were counted by two high-purity Ge detectors for low-energy photons (Ge_1, Ge_2). The aperture of the C_0 collimator was 2 mm. A free air ion chamber (FAIC) was located in front of the sample to monitor incident photon intensity. The sample was placed at point O; its normal vector is $(-\frac{1}{2}, -\frac{1}{\sqrt{2}}, \frac{1}{2})$. Collimators$(C_1, C_2)$ define the opening angle of Ge Detectors. The distance from the surface of the sample to the exit of collimator (L_1) was 434 mm and the aperture of Collimator(D_1) was 5.01 mm.

2) Comparison of the photon spectra scattered by the C and Cu samples. The measured and calculated values are shown in symbols and histograms, respectively($k_0 = 40keV$, $\theta = 90°$). The EGS4 calculation with all of the modifications in this work, including Doppler broadening, is shown as EGS4(CP). The EGS4 calculation with all the modifications in this work, except for Doppler broadening, is shown as EGS4(S). The peak at 30keV is the Ge K X-ray escape peak of the Rayleigh-scattering peak at 40keV.

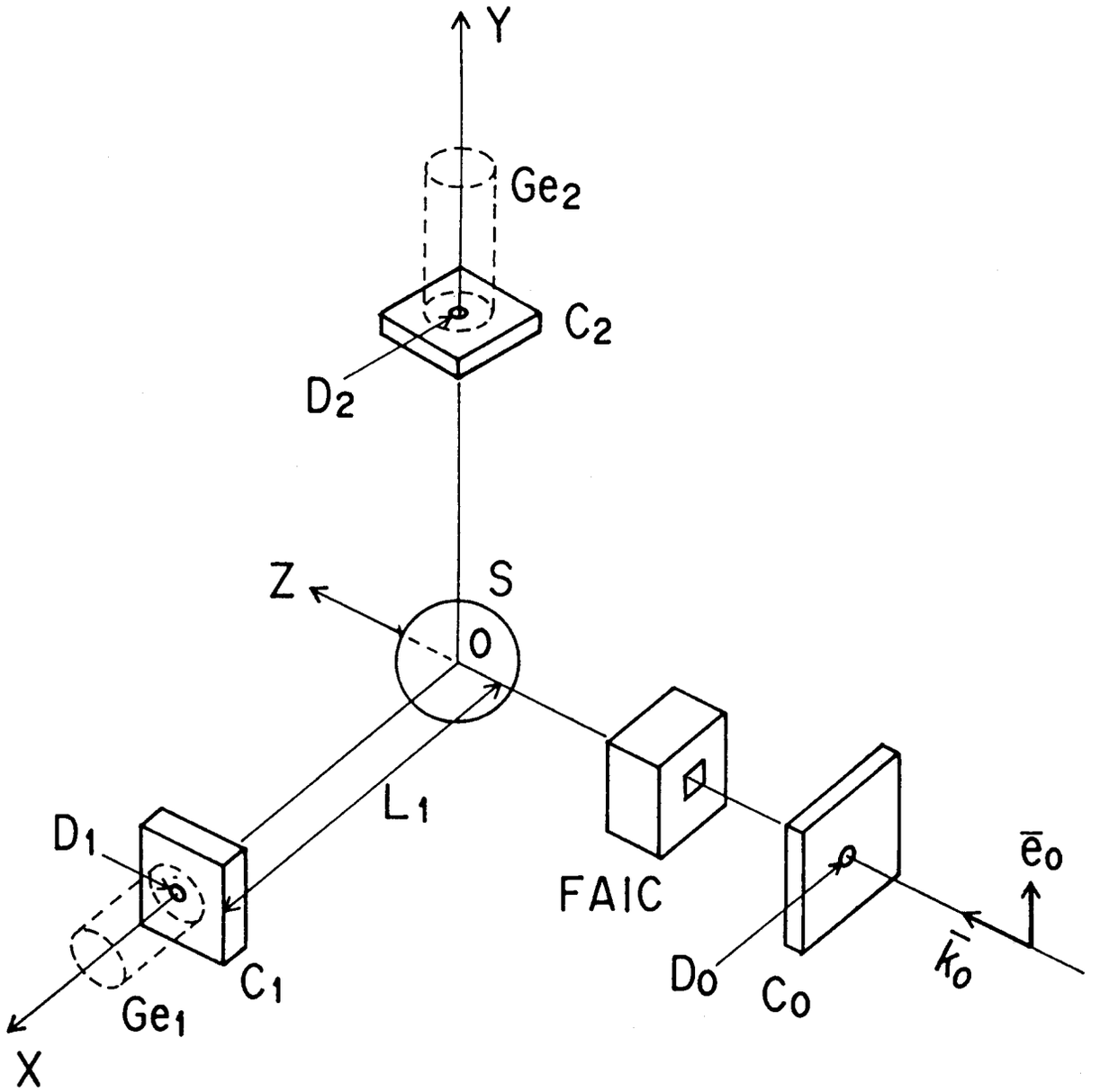

Fig.1

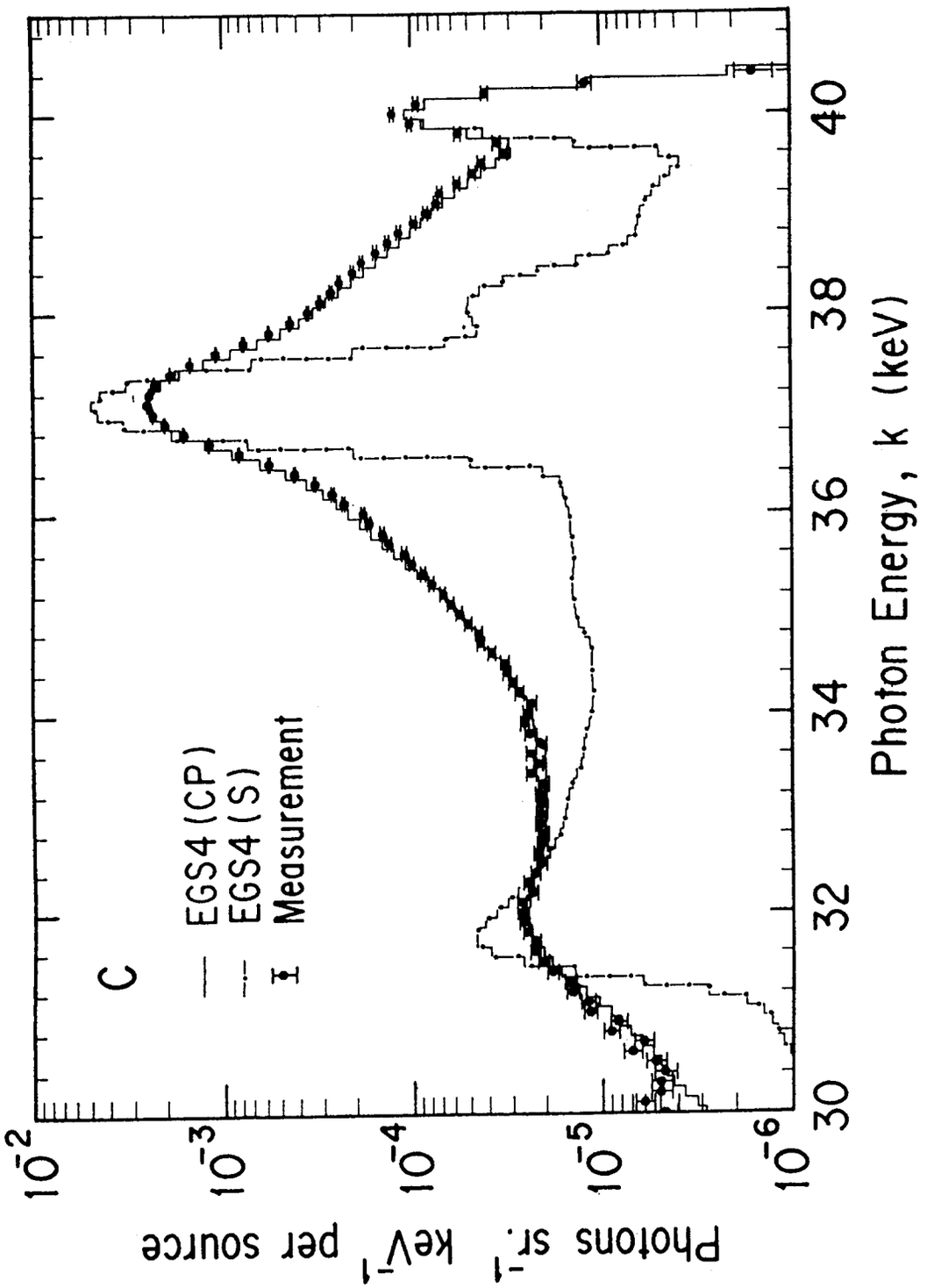
C
EGS4 (CP)
EGS4 (S)
Measurement
Photons sr⁻¹ keV⁻¹ per source
Photon Energy, k (keV)
10⁻²
10⁻³
10⁻⁴
10⁻⁵
10⁻⁶
30
32
34
36
38
40

Fig.2(a)

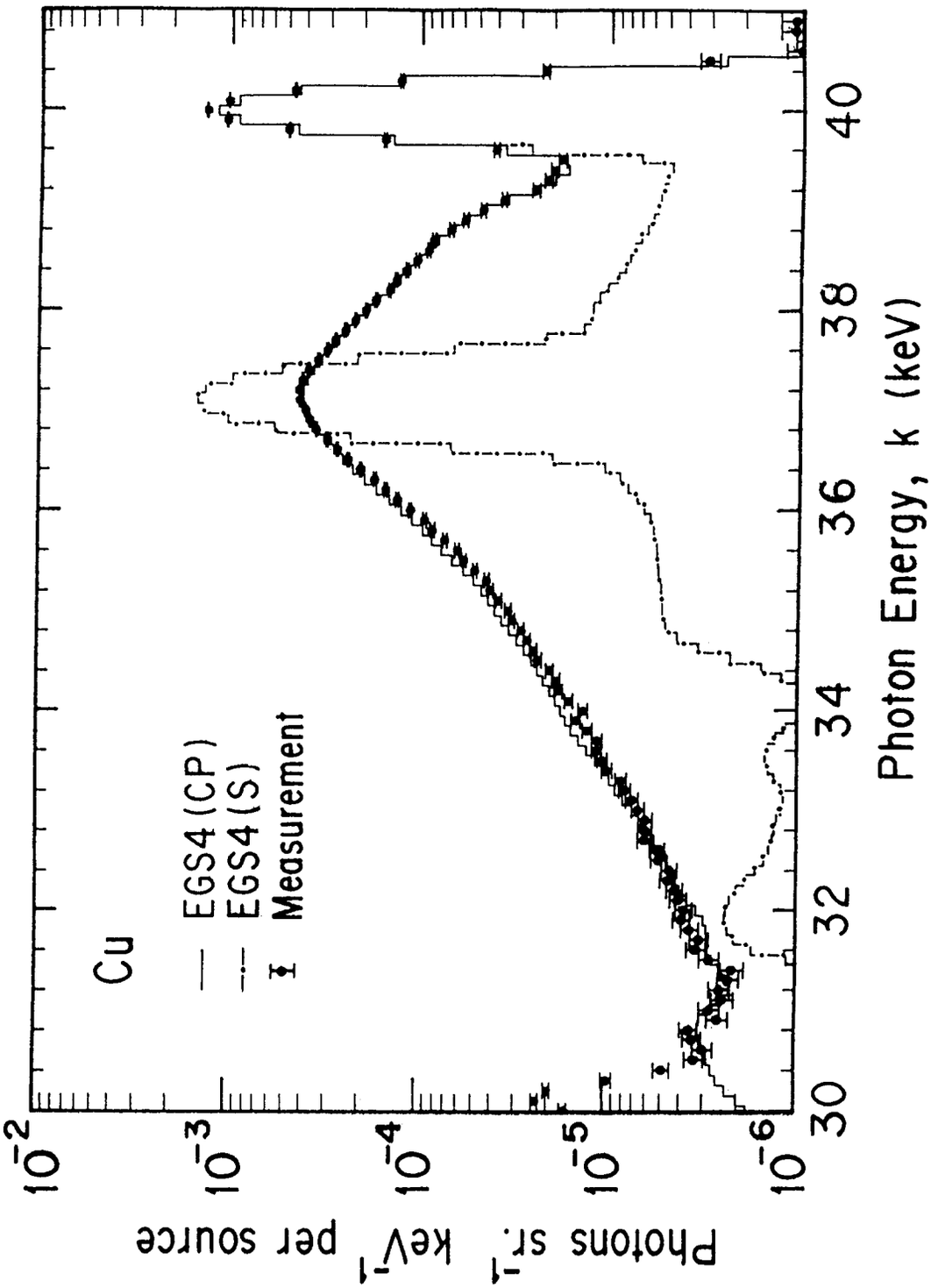
Cu
EGS4 (CP)
EGS4 (S)
Measurement
Photons sr⁻¹ keV⁻¹ per source
Photon Energy, k (keV)
10⁻²
10⁻³
10⁻⁴
10⁻⁵
10⁻⁶
30
32
34
36
38
40

Fig.2(b)